Quantum Light-Matter Interaction in Superconducting Circuits

Lecture note for the 14th School of Mesoscopic Physics

Myung-Joong Hwang*

Division of Natural and Applied Sciences, Duke Kunshan University, Kunshan, Jiangsu 215300, China

Disclaimer: This note is intended only as a brief companion to my lecture and has not been thoroughly proofread. It may contain errors or inaccuracies, so please use it with discretion.

Contents

I. OUTLINE

This lecture introduces the fundamental principles of quantum light-matter interaction, with a focus on the framework of circuit quantum electrodynamics (cQED), where microwave photons interact with matter degrees of freedom. We begin by discussing the quantization of the electromagnetic field in a microwave resonator. Building on this foundation, we explore the physics of light-matter interaction

The first example is the electric dipole interaction between a transmon qubit and microwave photons. We derive the Jaynes-Cummings model as an effective description of this system and discuss both the resonant and dispersive regimes. These regimes form the basis for coherent control and high-fidelity measurement of superconducting qubits. The second example involves magnetic dipole coupling between magnons and microwave photons, forming the basis of cavity quantum magnonics. We will see how quantum states of collective magnetic excitations can be prepared and probed via their interaction with microwave photons.

Through these examples, we aim to illustrate how different physical platforms harness quantum electromagnetic fields to control and study quantum systems.

II. QUANTIZATION OF ELECTROMAGNETIC FIELD

A standard approach to quantizing the electromagnetic field begins by constructing a Lagrangian that reproduces Maxwell's equations. From this, one identifies the conjugate variables and constructs the corresponding Hamiltonian.

---

*Electronic address: `myungjoong.hwang@duke.edu`

By expressing the field in terms of its normal modes, whose commutation relations follow the canonical bosonic form, one arrives at the non-interacting Hamiltonian for the photonic modes:

$$H_{\text{pho}} = \sum_k \omega_k a_k^\dagger a_k. \tag{1}$$

Here, the operators $a_k^\dagger$ and a_k create and annihilate, respectively, a photon with frequency ω_k. A detailed treatment of electromagnetic field quantization can be found in standard textbooks such as Ref. [1].

In mesoscopic systems, the electromagnetic field is often supported by electrical circuits. In such cases, it is convenient to work with circuit variables such as charge, flux, voltage, and current. The quantization procedure follows the same basic steps: (a) construct a Lagrangian that yields the equations of motion for the circuit under consideration, (b) identify the conjugate variables and construct the corresponding Hamiltonian, and (c) impose canonical commutation relations on the normal modes of the conjugate variables. This leads to a bosonic Hamiltonian describing non-interacting photons, as above.

This circuit-based quantization scheme for the electromagnetic field will be introduced in this lecture.

A. Circuit quantization of a lumped LC oscillator

An electrical circuit can be analyzed with the current and the voltage drop across the circuit elements, or equivalently, with a time integral of the current and voltage variable. The equation of motion is obtained from the usual Kirchkoff's law. Consider a simple LC oscillator in Fig. 1. A variable we use to describe the oscillator is the flux Φ, defined as

$$\Phi(t) = \int_{-\infty}^{t} V(t')dt' \tag{2}$$

A sign convention for the current and the voltage is following: For an element with a node 1 and 2, a positive current direction is from the node 1 to 2, while the voltage drop is defined as the voltage difference from the node 2 to 1. For example, in Fig. 1, for the current I flowing from the ground to the node Φ (the red dot), the associated voltage drop is the voltage difference between the red dot and the ground, $V - 0$. Using this sign convention, we express the current through the inductor and capacitor,

$$I_L = \frac{\Phi - 0}{L} = \frac{\Phi}{L}, \quad I_C = C(\dot{V} - 0) = C\ddot{\Phi} \tag{3}$$

From the Kirchhoff's law, $I_C + I_L = 0$, the equation of motion is

$$C\ddot{\Phi} + \frac{\Phi}{L} = 0. \tag{4}$$

The classical Lagrangian that gives the above equation of motion,

$$\mathcal{L} = \frac{C\dot{\Phi}^2}{2} - \frac{\Phi^2}{2L} \tag{5}$$

This is nothing but a harmonic oscillator with the flux variable Φ as a position coordinate. The momentum conjugate variable, Q, is then,

$$Q = \frac{\partial \mathcal{L}}{\partial \dot{\Phi}} = C\dot{\Phi} \tag{6}$$

We construct the Hamiltonian from the Legendre transformation,

$$H = Q\dot{\Phi} - \mathcal{L} = \frac{Q^2}{2C} + \frac{\Phi^2}{2L} \tag{7}$$

and finally, we impose a the canonical commutation relation ($[x, p] = i\hbar$), and treat the variables as operators,

$$[\hat{\Phi}, \hat{Q}] = i\hbar \tag{8}$$

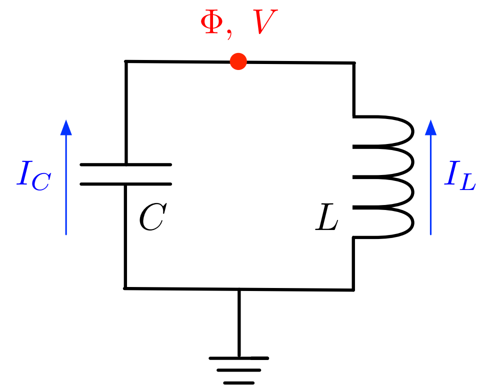

FIG. 1: A lumped LC oscillator.

$$H = \frac{\hat{Q}^2}{2C} + \frac{\hat{\Phi}^2}{2L} \tag{9}$$

We proceed by defining the usual creation and annihilation operators. Recall that for the harmonic oscillator $H = \frac{p^2}{2m} + \frac{mw^2}{2}x^2$, the zero point fluctuation are $x_{ZPF} = \sqrt{\frac{\hbar}{2mw}}$ and $p_{ZPF} = \sqrt{\frac{\hbar mw}{2}}$. The zero point fluctuation of the flux and the conjugate variable is then,

$$\Phi_{ZPF} = \sqrt{\frac{\hbar Z}{2}}, \quad Q_{ZPF} = \sqrt{\frac{\hbar}{2Z}} \tag{10}$$

where $Z = \sqrt{L/C}$ is the characteristic impedance of the LC oscillator. Using these, we define the Φ and Q using a dimensionless creation and annihilation operators,

$$\hat{\Phi} = \Phi_{ZPF}(a + a^\dagger), \quad \hat{Q} = iQ_{ZPF}(a^\dagger - a) \tag{11}$$

Then, the Hamiltonian becomes

$$H = \hbar\omega_0(a^\dagger a + \frac{1}{2}) \tag{12}$$

with $\omega_0 = 1/\sqrt{LC}$. The excitations of the LC circuit can be regarded as photons. We call this as a lumped LC oscillator because the typical wavelength of the $\frac{2\pi c}{\omega_0}$, which is around centimeters, is much longer than the size of the circuit, typically in micrometers. In next section, we will deal with a different kind of LC oscillator where the size of circuits is also a centimeter long so that the lumped approximation cannot hold anymore.

B. Quantization of coplanar microwave cavity

Now we consider a coplanar waveguide of length 2ℓ with a capacitance of $2\ell C_0$ and an inductance $2\ell L_0$. Here, C_0 and L_0 are defined as capacitance and inductance per unit length. The coplanar waveguide can be modeled as a series of LC oscillator as shown in Fig. 2. We start with setting up the equation of motion. The current flowing out of the node n is given by

$$I_{n+1,L_0} = \frac{\Phi_{n+1} - \Phi_n}{L_0 \Delta x} \tag{13}$$

where Δx is the length of the distributed inductor. On the other hand, the current flowing into the node has a contribution both from the inductor and capacitor,

$$I_{n,L_0} = \frac{\Phi_n - \Phi_{n-1}}{L_0 \Delta x}, \qquad I_{n,C_0} = C_0 \Delta x \ddot{\Phi}_n \tag{14}$$

From the Kirchhoff's law, $I_{n,L_0} + I_{n,C_0} = I_{n+1,L_0}$, the equation of motion is

$$C_0 \Delta x \ddot{\Phi}_n = \frac{\Phi_{n+1} - 2\Phi_n + \Phi_{n-1}}{L_0 \Delta x} \tag{15}$$

The Lagrangian that gives rise to the above equation of motion is,

$$\mathcal{L} = \sum_n \left[\frac{C_0 \Delta x \dot{\Phi}_n^2}{2} - \frac{(\Phi_n - \Phi_{n-1})^2}{2L_0 \Delta x} \right] \tag{16}$$

By consdering the continuum limit, $\Delta x \to 0$, the Lagrangian becomes

$$\mathcal{L} = \int_{-\ell}^{\ell} dx \left[\frac{C_0 \dot{\Phi}(x)^2}{2} - \frac{(\partial_x \Phi(x))^2}{2L_0} \right] \tag{17}$$

with the equation of motion

$$\ddot{\Phi}(x) = \frac{1}{C_0 L_0} \partial_x^2 \Phi(x) \tag{18}$$

which is simply a wave equation with a velocity $v = 1/\sqrt{L_0 C_0}$. Note also that the current and voltage at x is given by

$$I(x) = \frac{\partial_x \Phi(x)}{L_0} \tag{19}$$

$$V(x) = \dot{\Phi}(x). \tag{20}$$

The boundary condition is given by vanishing current at the end of the central conductor, namely,

$$\partial_x \Phi(x)|_{\ell} = \partial_x \Phi(x)|_{-\ell} = 0 \tag{21}$$

Now, what we need to do is to find a normal mode of the system. We express the flux variable in terms of normal modes,

$$\Phi(x,t) = \sum_{n=1}^{\infty} \psi_n(t) v_n(x) \tag{22}$$

which satisfy

$$\ddot{\psi}_n(t) = -w_n^2 \psi_n(t), \quad \partial_x^2 v_n(x) = -k_n^2 v_n(x) \tag{23}$$

with $w_n = k_n v$. By imposing the bound condition (Eq. 21), we can solve the above equation and get

$$v_n(x) = \sqrt{\frac{1}{\ell}} \cos[k_n(x+\ell)] \tag{24}$$

where $k_n = \frac{\pi n}{2\ell}$ and the normalization condition is imposed;

$$\int_{-\ell}^{\ell} v_m(x) v_n(x) dx = \delta_{nm} \tag{25}$$

With the normal mode, the Lagrangian can be diagonalized,

$$\mathcal{L} = \sum_n \left(\frac{C_0}{2} \dot{\psi}_n^2 - \frac{1}{2L_0} k_n^2 \psi_n^2 \right) \tag{26}$$

$$= \frac{C_0}{2} \sum_n \left(\dot{\psi}_n^2 - w_n^2 \psi_n^2 \right) \tag{27}$$

Finally, we define the charge conjugate variable,

$$\theta_n = \frac{\partial \mathcal{L}}{\partial \dot{\psi}_n} = C_0 \dot{\psi}_n \tag{28}$$

from which we obtain the Hamiltonian

$$H = \sum_n \left(\frac{1}{2C_0}\theta_n^2 + \frac{C_0}{2} w_n^2 \psi_n^2\right) \tag{29}$$

Then, we impose the canonical commutation relation

$$[\hat{\psi}_m, \hat{\phi}_n,] \;=\; i\hbar\delta_{nm}$$

The coefficient of the Hamiltonian in Eq. 29 is arranged in a way that one can directly guess the zero point fluctuation of the flux and the charge variables, and define the dimensionless creation and annihilation operators,

$$\hat{\psi}_n = \psi_{ZPF}(\hat{a}_n + \hat{a}_n^\dagger) \tag{30}$$

$$\hat{\theta}_n = i\theta_{ZPF}(\hat{a}_n^\dagger - \hat{a}_n) \tag{31}$$

where

$$\psi_{ZPF} = \sqrt{\frac{\hbar}{2C_0 w_n}} = \sqrt{\frac{\hbar Z}{2k_n}} \tag{32}$$

$$\theta_{ZPF} = \sqrt{\frac{C_0 \hbar w_n}{2}} = \sqrt{\frac{\hbar k_n}{2Z}} \tag{33}$$

where the characteristic impedance $Z = \sqrt{L_0/C_0}$. We now arrive at the quantized Hamiltonian of the transmission line,

$$H = \sum_n \hbar\omega_n (\hat{a}_n^\dagger \hat{a}_n + \frac{1}{2}) \tag{34}$$

with$[a_n, a_m^\dagger] = 1$. In circuit QED, we can utilize a capacitive coupling or inductive coupling to the superconducting qubit, depending on the flavor of the qubit of interest. In this case, we need to know express the flux or charge variables at the point where the field couples to the qubit. Therefore, in terms of the normal mode, they are

$$\hat{\Phi}(x) = \psi_{ZPF} \sum_n (a_n + a_n^\dagger) v_n(x) \tag{35}$$

$$\hat{Q}(x) = i\theta_{ZPF} \sum_n (a_n^\dagger - a_n) v_n(x) \tag{36}$$

The voltage and current operators will also be found useful, and they can be obtained using $\hat{V}(x) = \frac{\hat{Q}}{C_0}$ and $\hat{I}(x) = \partial x \hat{\Phi}(x)$,

$$\hat{V}(x) = i\sqrt{\frac{\hbar w_n}{2C_0}} \sum_n (a_n^\dagger - a_n) v_n(x) \tag{37}$$

$$\begin{aligned} \hat{I}(x) &= \psi_{ZPF} \sum_n (a_n + a_n^\dagger) \sqrt{\frac{1}{\ell}} (-k_n) \sin[k_n(x+\ell)] \\ &= -\sqrt{\frac{\hbar L_0 \hbar w_n}{2\ell}} \sum_n (a_n + a_n^\dagger) \sin[k_n(x+\ell)] \end{aligned} \tag{38}$$

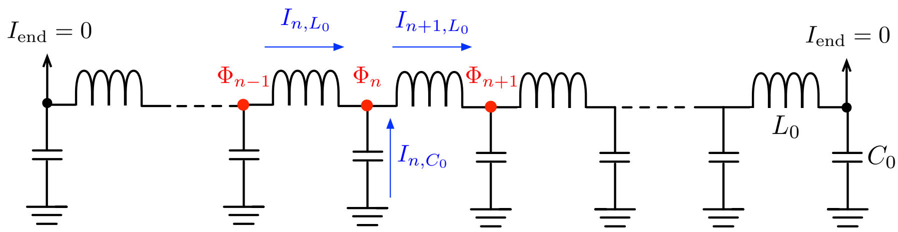

FIG. 2: A microwave cavity made out of a 2D transmission line can be modeled as a distributed LC circuit.

III. CIRCUIT QED - ELECTRIC DIPOLE INTERACTION BETWEEN MICROWAVE PHOTONS AND TRASMON QUBIT

A. Transmon

A Josephson junction can be understood as a non-linear inductor whose potential energy is given by

$$E_J = -E_J \cos(2\pi \frac{\hat{\Phi}}{\Phi_0}). \tag{39}$$

where E_J is the Josephson energy and $\Phi_0 = h/2e$ is the flux quantum. A cooper pair box consists of the capacitor and the Josephson junction. We can write down the Hamiltonian for the cooper pair box with the knowledge of the lumped oscillator. From the Hamiltonian for the lumped LC oscillator, given in Eq. 7, we can simply replace the inductor part with the Josephson junction energy. That is,

$$H_{CPB} = \frac{(\hat{Q} - Q_g)^2}{2C_J} - E_J \cos(2\pi \frac{\hat{\Phi}}{\Phi_0}) \tag{40}$$

Note that we have added Q_g to change the potential minimum for the charge which can be controlled by a gate voltage $Q_g = C_g V_g$ or can be uncontrolled off-set charge. The commutation relation is still the same, $[\hat{\Phi}, \hat{Q}] = i\hbar$. Equivalently, we can define the number operator, $\hat{n} = \hat{Q}/(2e)$, and using the phase operator, $\hat{\phi} = 2\pi \frac{\hat{\Phi}}{\Phi_0}$, and re-express the Hamiltonian,

$$H_{CPB} = 4E_C(\hat{n} - n_g)^2 - E_J \cos(\hat{\phi}) \tag{41}$$

where $E_C = e^2/(C_J + C_g)$.

The transmon operates at a parameter regime $E_J \gg E_C$. Namely, the Josephson energy dominates over the charging energy and therefore the number of charge has a large fluctuation in the eigenstates. Therefore, the gate voltage has little effect in the energy eigenstates, which translates into an insensitivity to charge noise and a increased coherence time, compared to a charge qubit which operates in an opposite limit $E_C \gg E_J$. The phase fluctuation for transmon, on the other hand, is highly suppressed and therefore it is possible to expand the cosine potential around the potential minimum $\phi = 0$, leading to

$$H_{\text{transmon}} = 4E_C \hat{n}^2 + \frac{E_J}{2}\hat{\phi}^2 - \frac{E_J}{4!}\hat{\phi}^4 \tag{42}$$

The quadratic part of the Hamiltonian is just a harmonic oscillator like the lumped LC oscillator case, and it can be diagonalized using

$$\hat{\phi} = \left(\frac{2E_C}{E_J}\right)^{1/4} (\hat{a} + \hat{a}^\dagger) \tag{43}$$

and

$$\hat{n} = \frac{i}{2}\left(\frac{E_J}{2E_C}\right)^{1/4} (\hat{a}^\dagger - a) \tag{44}$$

where $[\hat{a}, \hat{a}^\dagger] = 1$. The transmon Hamiltonian is then a non-linear harmonic oscillator with a quartic potential, which reads

$$H_{\text{transmon}} = \sqrt{8E_J E_C}\hat{a}^\dagger\hat{a} - \frac{E_J}{12}(\hat{a} + a)^4 \tag{45}$$

Exercise 1. Find the typical values for the Josephson energy E_J and the charging energy E_C of the transmon qubit realized in any recent experiments. Estimate the anharmonicity of the energy spectrum by calculating numerically the energy difference between the first excited state and the ground state ($E_1 - E_0$) and the energy difference between the second excited state and the first excited state ($E_2 - E_1$).

Thanks to the anharmonicity in the energy spectrum estimated above, the system can be approximated as a two-level system by truncating to the lowest two energy levels, enabling its use as a qubit. While the probability of exciting higher energy levels is small, it is not negligible and constitutes an important source of error in qubit operations, known as leakage error.

B. Capacitive coupling between the microwave resonator and the transmon

A transmon, consisting of two superconducting islands connected by a Josephson junction, can be regarded as an electric dipole. When placed inside a microwave resonator, the transmon interacts with the resonator through electric dipole coupling. In the case of a lumped-element LC resonator, this interaction can be modeled as a capacitive coupling mediated by a coupling capacitor C_c. The corresponding charging energy takes the form

$$H_{\text{int}} = 8E_{C_c}\hat{n}_{\text{res}}\hat{n}_{\text{trans}}, \tag{46}$$

where terms proportional to $\hat{Q}^2_{\text{res}}$ and $\hat{Q}^2_{\text{trans}}$ are neglected, as they merely renormalize the capacitances of the resonator and the transmon, respectively. Using Eq. 44, and denoting the boson operator for the resonator $\hat{a}$ and for the transmon $\hat{b}$, respectively, the interaction Hamiltonian reads

$$H_{\text{int}} = -2E_{C_c}\left(\frac{E_{\text{J,res}}}{2E_{\text{C,res}}}\right)^{1/4}\left(\frac{E_{\text{J,trans}}}{2E_{\text{C,trans}}}\right)^{1/4}(\hat{a}^\dagger - \hat{a})(\hat{b}^\dagger - \hat{b}) \tag{47}$$

After the two-level approximation for the transmon, we can replace $\hat{b}$ ($\hat{b}^\dagger$) with the pauli operaltor σ_- (σ_+). Let's also denote the coupling energy given above as $\hbar\lambda$. Then, we arrive at the so-called quantum Rabi model,

$$H_{QRM} = \omega_0 a^\dagger a + \frac{1}{2}\Omega\sigma_z - \lambda(a^\dagger - a)(\sigma_+ - \sigma_-). \tag{48}$$

Note that we have set $\hbar = 1$ for convenience. The interaction Hamiltonian can be divided into

$$H_{int} = \lambda\left(a\sigma_+ + a^\dagger\sigma_-\right) + \lambda\left(a\sigma_- + a^\dagger\sigma_+\right) \tag{49}$$

The second term create or annihilate an energy quanta from the qubit and the field at the same time. These terms are called counter rotating terms. If the coupling strength g is much smaller than the cavity frequency ω_0, this term can be neglected by the so-called rotating wave approximation. A typical energy scale for the circuit QED systems with a transmon qubit indeed satisfy this condition. Namely, ω_0 and Ω is in the range of a few GHz, while g is in the order of 100 MHz.

C. Jaynes-Cummings Hamiltonian

After neglecting the conter rotating terms, the circuit QED Hamiltonian becomes the Jaynes-Cummings Hamiltonian

$$H_{JC} = \omega_0 a^\dagger a + \frac{1}{2}\Omega\sigma_z + \lambda\left(a\sigma_+ + a^\dagger\sigma_-\right) \tag{50}$$

The JC Hamiltonian has a conserved quantity. Consider

$$M = a^\dagger a + \frac{1}{2}\sigma_z \tag{51}$$

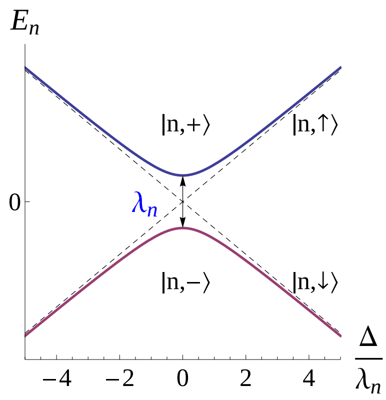

FIG. 3: Eigenvalues of the nth block of the Jaynes-Cummings Hamiltonian

which represents a total number of excitation. Notice

$$[M, H_{JC}] = 0\,, \tag{52}$$

so that the total number of excitation is preserved. Therefore the Hamiltonian can be block-diagonalized into subspaces spanned by states with a same number of excitations, that is, $|n,\uparrow\rangle$ and $|n+1,\downarrow\rangle$.

$$H \doteq \left[\begin{array}{c|cccc} H & \cdots & |n,\uparrow\rangle & |n+1,\downarrow\rangle & \cdots \\ \hline \vdots & \ddots & & & \\ \langle n,\uparrow| & & n\omega_0 + \frac{1}{2}\Omega & \lambda\sqrt{n+1} & \\ \langle n+1,\downarrow| & & \lambda\sqrt{n+1} & (n+1)\omega_0 - \frac{1}{2}\Omega & \\ \vdots & & & & \ddots \end{array}\right], \tag{53}$$

The nth block Hamiltonian can be written in terms of a pseudo spin

$$H_n = \omega_0\left(n + \frac{1}{2}\right)\tau_0 + \frac{1}{2}\left\{\Delta\,\tau_z + 2\lambda\sqrt{n+1}\tau_x\right\}\,, \tag{54}$$

where τ_μ ($\mu = 0, x, y, z$) are (pseudo-spin) Pauli matrices and $\Delta = \Omega - \omega_0$. The eigenvalues are

$$E_\pm(n) \;=\; \omega_0\left(n + \frac{1}{2}\right) \pm \frac{1}{2}\sqrt{(1+n)(2\lambda)^2 + \Delta^2} \tag{55}$$

$$\;=\; \omega_0\left(n + \frac{1}{2}\right) \pm \frac{1}{2}\sqrt{\lambda_n^2 + \Delta^2} \tag{56}$$

where $\lambda_n \equiv 2\lambda\sqrt{n+1}$. See Fig. 3for the energy as a function of the detuning Δ. The corresponding eigenvectors are

$$|n,+\rangle = +\cos(\theta_n/2)\,|n,\uparrow\rangle + \sin(\theta_n/2)\,|n+1,\downarrow\rangle\,, \tag{57}$$

$$|n,-\rangle = -\sin(\theta_n/2)\,|n,\uparrow\rangle + \cos(\theta_n/2)\,|n+1,\downarrow\rangle\,, \tag{58}$$

where $\tan\theta_n \equiv (2\lambda/\Delta)\sqrt{n+1}$.

D. Vacuum Rabi oscillation

At resonance, $\Delta = 0$, the eigenstates are

$$|n,+\rangle = \frac{1}{\sqrt{2}}(|n,\uparrow\rangle + |n+1,\downarrow\rangle)\,, \tag{59}$$

$$|n,-\rangle = \frac{1}{\sqrt{2}}(-\,|n,\uparrow\rangle + |n+1,\downarrow\rangle)\,. \tag{60}$$

and the energy difference between the two states is

$$\lambda_n = 2\lambda\sqrt{n+1} \tag{61}$$

Therefore, if one prepare an initial state $|n,\uparrow\rangle$, the state will oscillate between $|n,\uparrow\rangle$ and $|n+1,\downarrow\rangle$ at a frequency, λ_n. This holds true even when initially there is no photon inside of the cavity. That is if one prepare a state, $|0,\uparrow\rangle$, the cavity and the atom can exchange an energy quanta at a frequency, 2λ, and this is called a vacuum Rabi frequency. This is a smoking gun feature of a coherent interaction between the cavity field and the atom.

E. Dispersive limit and qubit measurement

A dispersive limit is where the detuning between the photon frequency and the qubit frequency $\Delta \equiv |\omega_0 - \Omega|$ is larger than the coupling strength, namely,

$$\frac{\lambda}{|\omega_0 - \Omega|} \ll 1 \qquad \text{(dispersive limit)}. \tag{62}$$

To find approximation to the Jaynes-Cummings Hamiltonian in the dispersive limit, one could apply the Schrieffer-Wolff transformation that makes the Hamiltonian diagonal in the spin and photon basis.

$$H_{\text{dispersive}} = \omega_0 a^\dagger a + \frac{\Omega}{2}\sigma_z + \frac{\lambda^2}{\Delta} a^\dagger a \sigma_z. \tag{63}$$

> **Exercise 2.** Perform a Schrieffer-Wolff transformation on the JC Hamiltonian, Eq. 50, to derive the dispersive Hamiltonian given in Eq. 63.

The physical interpretation of the dispersive interaction term $\frac{\lambda^2}{\Delta} a^\dagger a \sigma_z$ is two-fold. The first is that the photon frequency is shifted up or down depending on the spin state, namely,

$$\omega_0 \to \omega_0 + \frac{\lambda^2}{\Delta} \quad \text{(for spin up)}, \quad \omega_0 \to \omega_0 - \frac{\lambda^2}{\Delta} \quad \text{(for spin down)}. \tag{64}$$

Therefore, one can measure the qubit state by measuring the frequency of the cavity. This is a standard way of measuring the transmon qubit. The second way to understand is that the transition frequency of the qubit depends on the number of photons in populated in the cavity, namely,

$$\Omega \to \Omega + \frac{\lambda^2}{\Delta} n \tag{65}$$

where n is the number of cavity photons. This interaction is useful for measuring the photon number distribution of the cavity field.

> **Exercise 3.** It turns out that the dispersive shift λ^2/Δ obtained above does not accurately predict the frequency shift observed in typical transmon experiments. This discrepancy arises because the two-level approximation is applied to the transmon Hamiltonian in Eq. 45 prior to calculating the dispersive shift. To address this limitation, consider a cQED Hamiltonian
>
> $$H = \omega_0 a^\dagger a + \omega_{\text{trans}} b^\dagger b - \frac{E_J}{2} b^\dagger b^\dagger b b + g(a b^\dagger + a^\dagger b) \tag{66}$$
>
> Note that among the quartic terms $(b + b^\dagger)^4$, only the terms that contain the same number of b and $b^\dagger$, since the other terms will be fast rotating terms and can be neglected with RWA. Construct a Schrieffer-Wolff transformation to transform the Hamiltonian into the dispersive form,
>
> $$H_{\text{dispersive}} = \omega_0' a^\dagger a + \frac{\Omega'}{2}\sigma_z + \chi' a^\dagger a \sigma_z, \tag{67}$$
>
> and find the expression for the renormalized frequencies ω_0' and Ω' and the dispersive shift χ'. Compare your results with Ref. [2].

IV. CAVITY MAGNONICS - MAGNETIC DIPOLE INTERACTION BETWEEN MICROWAVE PHOTONS AND MAGNONS

In the previous section, we examine how the electric field component of the microwave photons couples to the transmon qubit. Another way of realizing the light-matter interaction is the magnetic dipole interaction. Here I will give a brief introduction to one example of cavity magnonics setup introduced in Ref. [3]. See Fig. IV B(a) for schematics of the setup, which consists of an easy-axis ferromagnetic insulator subject to an external static magnetic field, placed inside of a microwave cavity. Its low-energy excitations can be modeled with the Hamiltonian,

$$\mathcal{H}_{\mathrm{tot}} = \omega b^\dagger b - \frac{g}{\sqrt{N}}\sqrt{\frac{2}{S}}(b + b^\dagger)\sum_{\boldsymbol{r}} \hat{S}^z_{\boldsymbol{r}} + \mathcal{H}_{\mathrm{FM}}, \tag{68}$$

with the spin Hamiltonian part of the ferromagnet,

$$\mathcal{H}_{\mathrm{FM}} = -J\sum_{\langle \boldsymbol{r},\boldsymbol{r'}\rangle} \hat{\boldsymbol{S}}_{\boldsymbol{r}} \cdot \hat{\boldsymbol{S}}_{\boldsymbol{r'}} - \sum_{\boldsymbol{r}} (K\hat{S}^{z2}_{\boldsymbol{r}} + \gamma\mu \boldsymbol{H}\cdot\hat{\boldsymbol{S}}_{\boldsymbol{r}}), \tag{69}$$

where $g = \gamma\mu h\sqrt{NS/2}$ is the magnetic dipole coupling strength between the cavity field and the spins, N is the number of spins, $\hat{\boldsymbol{S}}_{\boldsymbol{r}}$ denotes the dimensionless spin of magnitude S at site $\boldsymbol{r}$, b is a bosonic operator of the cavity field with the frequency ω and the strength h, μ is the permeability, and $\boldsymbol{H}$ is the static field. $J > 0$ denotes the Heisenberg-type isotropic ferromagnetic exchange interaction between the neighboring sites, $K > 0$ represents the easy-axis anisotropy along the z axis, and γ is the gyromagnetic ratio for the Zeeman interaction. J has the dominant energy scale responsible for the ferromagnetic spin ordering, whose direction is determined by the competition between K, $\boldsymbol{H}$, and g with weak characteristic energy scales.

A. Magnon Hamiltonian

Exercise 4. Suppose the magnetic field $\boldsymbol{H} = H_0\hat{y}$ is sufficiently strong such that the magnetization of the ferromagnet aligns along the y-axis. Diagonalize the spin Hamiltonian $\mathcal{H}_{\mathrm{FM}}$ by performing the following steps: (a) apply the Holstein–Primakoff transformation to express spin operators in terms of bosonic operators, retaining only linear terms under the low-excitation approximation; (b) perform a Fourier transformation of the bosonic operators to define magnon modes in momentum space; and (c) apply a Bogoliubov transformation to diagonalize the resulting quadratic magnon Hamiltonian. Compare your results with Ref. [3].

The resulting magnon Hamiltonian obtained through Exercise 4 can be written as

$$H = \sum_k \Omega_k \tilde{m}^\dagger_k \tilde{m}_k. \tag{70}$$

where $\Omega_{\boldsymbol{k}} = 2\sqrt{A^2_{\boldsymbol{k}} - B^2}$ with

$$A_{\boldsymbol{k}} = JSn_1\zeta_{\boldsymbol{k}} + \frac{KS}{2}(2\chi - 1),\ B = \frac{KS}{2}, \tag{71}$$

Here, n_1 is the coordination number, $\zeta_{\boldsymbol{k}} = (1 - \frac{1}{n_1}\sum_{\pm\boldsymbol{\delta}} e^{i\boldsymbol{k}\cdot\boldsymbol{\delta}})$ and $\boldsymbol{\delta}$ is the displacement vector to the nearest neighbors. Note that the anisotropy term $K\hat{S}^{z2}_{\boldsymbol{r}}$ contains processes that simultaneously creates and annihilates two magnons, which is why one needs a Bogoliubov transformation to diagonalize the magnon Hamiltonian. These processes induces a magnon squeezing, which reduces the uncertainty of the magnon along a certain quadrature below the minimum uncertainty level. The degree of squeezing $r_{\boldsymbol{k}}$ is

$$r_{\boldsymbol{k}} = \log\left(\frac{A_{\boldsymbol{k}} + B}{A_{\boldsymbol{k}} - B}\right)^{1/4}. \tag{72}$$

B. Quantum optical measurement of magnon squeezing

The cavity magnonics Hamiltonian in Eq. 68 can now be written in terms of the magnonic Hamiltonian where we keep only the uniform magnonic (Kittle) mode $\tilde{m} = \tilde{m}_{\boldsymbol{k}=0}$, which coherently couples to the cavity field, reads

$$\mathcal{H}_{\mathrm{c}} = \Omega_0\tilde{m}^\dagger\tilde{m} + \omega b^\dagger b - i\tilde{g}(\tilde{m} - \tilde{m}^\dagger)(b + b^\dagger), \tag{73}$$

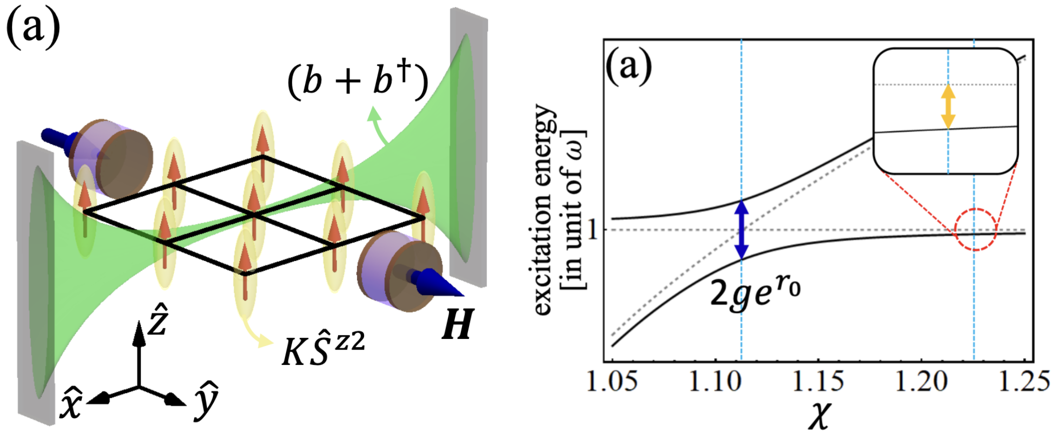

FIG. 4: [Adapted from Ref. [3]] (left) Schematic illustration of a cavity magnonics system. The green region enclosed by the rectangles, the arrows on the grid, and the cylinders represent the cavity field, the easy-axis ferromagnet, and the coil for the external field, respectively. (right) Excitation energies of cavity magnonics Hamiltonian as a function of $\chi = |\gamma\mu H_0|/2KS$ for a fixed coupling strength g. The blue and yellow arrows indicate the vacuum Rabi splitting and the dispersive cavity frequency shift, respectively. The dashed black line indicates the bare cavity and magnon frequencies without the interaction.

where $\Omega_0 = KS/\sinh 2r_0$ and

$$\tilde{g} = ge^{r_0}. \tag{74}$$

Note that the effective cavity-magnon coupling strength $\tilde{g}$ is exponentially enhanced by the magnonic squeezing parameter r_0. The enhancement stems from the competition between the easy-axis anisotropy and the Zeeman interaction.

The enhanced $\tilde{g}$ allows a quantum optical measurement of the squeezing and the large spin angular momentum of magnons. To this end, one can tune $\tilde{g}$ to realize the strong coupling regime where $\tilde{g}$ is larger than the cavity (magnon) decay rate, κ (Γ), but is still smaller than the cavity (magnon) frequency ω (Ω_0); namely, $\kappa, \Gamma \ll \tilde{g} \ll \omega, \Omega_0$. On resonance, $\omega \sim \Omega_0$, an avoided crossing occurs giving rise to the vacuum Rabi splitting $(\Delta\omega)$ that is determined by the magnon squeezing, i.e., $\Delta\omega \simeq 2ge^{r_0}$. In a dispersive limit, $g \ll |\omega - \Omega_0|$, the cavity frequency ω is shifted by $2g^2e^{2r_0}/\Delta\omega|_{g=0}$ where $\Delta\omega|_{g=0}$ is the detuning between the bare cavity and magnon frequencies. See the right panel of Fig. IV B for the vacuum Rabi splitting and the dispersive shift of the cavity magnonics system. Therefore, by measuring the frequency shift of the cavity field, which is a standard experimental tool in the cavity and circuit QED, one can probe the degree of magnon squeezing.

This example highlights the power of quantum optical approaches to quantum magnetism. By leveraging the light-matter interaction between the cavity field and collective spin excitations, one can access and measure quantum properties of magnons, such as squeezing. Introducing a transmon qubit into the cavity magnonics setup enables effective qubit-magnon interactions mediated by the cavity field. Drawing on the extensive toolbox developed in cavity QED, it becomes possible to coherently control and probe the quantum states of magnons.

[1] C. Cohen-Tannoudji, J. Dupont-Roc, and G. Grynberg, *Photons and Atoms* (Wiley, New York, 1989).
[2] J. Koch, T. M. Yu, J. Gambetta, A. A. Houck, D. I. Schuster, J. Majer, A. Blais, M. H. Devoret, S. M. Girvin, and R. J. Schoelkopf, “Charge-insensitive qubit design derived from the Cooper pair box,” Phys. Rev. A **76**, 042319 (2007).
[3] J. M. Lee, H.-W. Lee, and M.-J. Hwang, ”Cavity magnonics with easy-axis ferromagnets: Critically enhanced magnon squeezing and light-matter interaction,” Phys. Rev. B **108**, L241404 (2023).